

PCCP

Accepted Manuscript



This is an *Accepted Manuscript*, which has been through the Royal Society of Chemistry peer review process and has been accepted for publication.

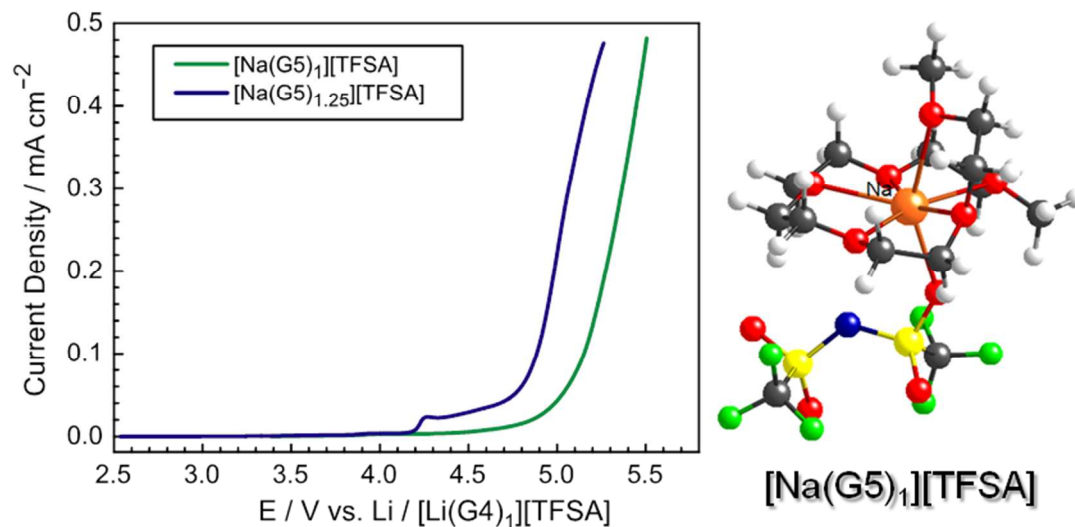
Accepted Manuscripts are published online shortly after acceptance, before technical editing, formatting and proof reading. Using this free service, authors can make their results available to the community, in citable form, before we publish the edited article. We will replace this *Accepted Manuscript* with the edited and formatted *Advance Article* as soon as it is available.

You can find more information about *Accepted Manuscripts* in the [Information for Authors](#).

Please note that technical editing may introduce minor changes to the text and/or graphics, which may alter content. The journal's standard [Terms & Conditions](#) and the [Ethical guidelines](#) still apply. In no event shall the Royal Society of Chemistry be held responsible for any errors or omissions in this *Accepted Manuscript* or any consequences arising from the use of any information it contains.

Table of Contents

Equimolar complex of pentaglyme (G5) and sodium bis(trifluoromethanesulfonyl)amide (Na[TFSA]) behaves like room-temperature ionic liquids and is a promising electrolyte for Na-ion batteries.



Physical Chemistry Chemical Physics: Article

Physicochemical Properties of Pentaglyme-Sodium Bis(trifluoromethanesulfonyl)amide Solvate Ionic Liquid

Shoshi Terada,[†] Toshihiko Mandai,[†] Risa Nozawa,[†] Kazuki Yoshida,[†]

Kazuhide Ueno,[†] Seiji Tsuzuki,[‡] Kaoru Dokko,^{†,§,} and Masayoshi Watanabe[†]*

[†]Department of Chemistry and Biotechnology, Yokohama National University,
79-5 Tokiwadai, Hodogaya-ku, Yokohama 240-8501, Japan

[‡]National Institute of Advanced Industrial Science and Technology (AIST),
Tsukuba Central 2, 1-1-1 Umezono, Tsukuba, Ibaraki 305-8568, Japan

[§]Unit of Elements Strategy Initiative for Catalysts & Batteries (ESICB), Kyoto University,
Kyoto 615-8510, Japan

AUTHOR EMAIL ADDRESS: dokko@ynu.ac.jp

RECEIVED DATE (to be automatically inserted after your manuscript is accepted if required according to the journal that you are submitting your paper to)

CORRESPONDING AUTHOR FOOTNOTE: To whom correspondence should be addressed. Telephone/Fax: +81-45-339-3942. E-mail: dokko@ynu.ac.jp

ABSTRACT

The physicochemical properties of pentaglyme (G5) and sodium bis(trifluoromethanesulfonyl)amide (Na[TFSA]) binary mixtures were investigated with respect to salt concentration and temperature. The density, viscosity, ionic conductivity, self-diffusion coefficient, and oxidative stability of a series of binary mixtures were measured, and the mixtures were examined as electrolytes for Na secondary batteries. An equimolar mixture of G5 and Na[TFSA] formed a low melting solvate, $[\text{Na}(\text{G5})_1][\text{TFSA}]$, which exhibited an ionic conductivity of 0.61 mS cm^{-1} at $30 \text{ }^\circ\text{C}$. The ionicity ($A_{\text{imp}}/A_{\text{ideal}}$) of the glyme-Na[TFSA] mixture was estimated from the molar conductivity of electrochemical impedance measurements (A_{imp}) and Walden plot (A_{ideal}). $[\text{Na}(\text{G5})_1][\text{TFSA}]$ possessed a high ionicity of 0.63 at $30 \text{ }^\circ\text{C}$, suggesting that $[\text{Na}(\text{G5})_1][\text{TFSA}]$ is highly dissociated into $[\text{Na}(\text{G5})_1]^+$ cation and $[\text{TFSA}]^-$ anion, regardless of extreme salt concentration in the liquid. The oxidative stabilities of G5–Na[TFSA] mixtures were investigated by linear sweep voltammetry, and the higher concentration resulted in higher oxidative stability due to the lowering of the HOMO energy level of G5 by complexation with Na^+ ion. In addition, battery tests were performed using the mixtures as electrolytes. The $[\text{Na} \mid [\text{Na}(\text{G5})_1][\text{TFSA}] \mid \text{Na}_{0.44}\text{MnO}_2]$ cell showed good charge–discharge cycle stability, with a discharge capacity of ca. 100 mA h g^{-1} , while the $[\text{Na}(\text{G5})_{1.25}][\text{TFSA}]$ system, containing excess G5, showed poor stability.

1. INTRODUCTION

Recently, Na secondary batteries have attracted much attention as promising post Li secondary batteries for realizing an energy sustainable society.^{1,2} The distribution of Li resources is limited to certain countries. On the other hand, Na is present in a large global abundance, primarily in seawater as NaCl salts, and hence, Na resources can be easily obtained at a lower cost compared to Li. The Na-S battery, which is composed of an elemental sulfur cathode, Na metal anode, and a proper solid-electrolyte, has been commercialized and utilized so far.³ However, since operating temperatures of this battery is as high as 300 °C at which both the sulfur cathode and Na anode are in the molten state, problems of safety arise for its utility in further diverse applications. Moreover, although some researchers reported the possibilities of Na secondary batteries,^{4–8} these systems often contain organic solvents as electrolytes, which may result in serious problems due to the flammability and volatility of electrolytes. With this in mind, Na secondary batteries that can be operated safely at ambient temperatures for prolonged periods are strongly desired.

Equimolar glyme-Li salt mixtures have recently emerged as promising alternatives to traditional organic electrolytes due to their remarkable physicochemical and electrochemical properties. In these mixtures, glymes, having the chemical structure of $\text{CH}_3\text{-O-(CH}_2\text{-CH}_2\text{-O)}_n\text{-CH}_3$ (especially, triglyme (G3; $n = 3$) and tetraglyme, (G4; $n = 4$)), coordinate to Li^+ cations to form long-lived complex cations in a 1:1 molar ratio.^{9–13} Appropriate combinations of glymes and Li salts result in molten liquid complexes at ambient temperature that behave like typical ionic liquids (ILs).¹⁴ Thus, they can be regarded as ILs consisting of complex $[\text{Li}(\text{glyme})_1]^+$ cations and counter anions, and can be further classified as “solvate ILs”.¹⁵ These complexes have sufficient ionic conductivity for use as an electrolyte and their oxidative and thermal stabilities are also considerably enhanced upon complexation. These fascinating properties allow glyme-Li solvate ILs to be used as electrolytes for Li secondary batteries with various cathode and anode materials.^{16–21}

On the basis of the similar chemical nature of congeners, glyme-Na salt molten complexes can be regarded as

one of the promising candidates of electrolytes for Na secondary batteries because of successful charge–discharge of Li secondary batteries using structurally analogous glyme-Li solvate IL electrolytes. Previously, we have systematically studied a series of glyme-Na salt binary mixtures with respect to phase diagrams and solvate structures, and found that they also exhibit the characteristics of equimolar complexes.²² Isothermal thermogravimetric analyses and temperature-dependent Raman spectra for the complexes have indicated that the characteristic solvate structures of certain glyme-Na salt equimolar complexes would be maintained even in the liquid state. Although the use of Na salt-IL binary mixtures, composed of Na salts and conventional aprotic ILs, as electrolytes has also been studied so far, they usually have serious drawbacks such as low Na⁺ ion transport properties mainly due to low Na⁺ ion concentration,^{23,24} resulting in poor battery performance at room temperature. In contrast, because glyme-Na salt equimolar complexes involve complex [Na(glyme)₁]⁺ ion as a single component cation, they can realize the relatively low viscous electrolytes with high Na⁺ ion concentration without any other media. These favorable characteristics strongly suggest the satisfactory potential of glyme-Na salt complexes as electrolytes for Na batteries. Among them, [Na(G5)₁][TFSA], the equimolar binary mixture of pentaglyme (G5) and sodium bis(trifluoromethanesulfonyl)amide salt (Na[TFSA]), is a likely candidate for this purpose because of exceptionally low crystallinity of this complex (the supercooled liquid state is easily formed at ambient temperature). However, there are no reports on the transport and electrochemical properties of [Na(G5)₁][TFSA] as an electrolyte.

In this paper, we report the physicochemical properties, including density, viscosity, and ionic conductivity, for a series of G5-Na[TFSA] binary mixtures as a function of concentration and temperature. On the basis of pulsed-field-gradient NMR spectroscopy, the ionic nature of the equimolar molten mixture, [Na(G5)₁][TFSA], was investigated. The oxidative stabilities of [Na(G5)_x][TFSA] were investigated by linear sweep voltammetry (LSV) accompanied with quantum chemical calculations. Furthermore, a battery test was performed to assess the performance of [Na(G5)₁][TFSA] electrolyte for Na secondary batteries.

2. EXPERIMENTAL SECTION

Materials

Bis(trifluoromethanesulfonyl)amine (H[TFSA]), Na₂CO₃, and 0.01 M KCl aqueous solution (standard) were purchased from TCI and used as received. Monoglyme (G1), diglyme (G2), and pentaglyme (G5) were supplied from Nippon Nyukazai. Triglyme (G3) and tetraglyme (G4) were purchased from TCI. All glymes except for G5 were distilled under high vacuum over sodium metal before use. G5 was used as received. The residual water contents in these liquids, measured by Karl Fischer titration, were less than 50 ppm. Acetylene black and poly(vinylidene fluoride) were purchased from Denki Kagaku Kogyo and Kishida Chemical, respectively, and used as received. All other chemicals and solvents were purchased from Wako Pure Chemical Industries, Ltd., and used without further purification. Na[TFSA] was synthesized by neutralization of H[TFSA] and Na₂CO₃ according to the previously published procedure.²⁵ The resulting Na[TFSA] was dried under high vacuum at 80 °C for 12 h and stored in an Ar-filled glove box until just before use. A series of [Na(G5)_x][TFSA] ($x = 0.8$ –3845) salts were prepared by mixing stoichiometric Na[TFSA] and G5 in the Ar-filled glove box with stirring for at least 12 h at 60 °C to achieve complete mixing.

The cathode active material for sodium batteries, Na_{0.44}MnO₂, was synthesized by a solid-state reaction according to the previously reported procedure.^{26, 27} Na₂CO₃ and MnCO₃ were manually ground using a mortar in a molar ratio of 0.48:2, pressed into pellets, and then heated for 8 h at 300 °C under air. The pellets were again ground into a powder using a mortar and pressed into pellets, followed by heating for 9 h at 800 °C under air.

Measurements

The thermal decomposition temperatures (T_d) for pure solvents and their mixtures with Na[TFSA] were evaluated by thermogravimetric (TG) measurements using a TG/DTA 6200 instrument (Seiko) from room

temperature to 550 °C at a heating rate of 10 °C min⁻¹ under a nitrogen atmosphere. Ionic conductivities (σ) of [Na(G5)_x][TFSA] were determined by the complex impedance method using an ac impedance analyzer (Princeton Applied Research, VMP3) in the frequency range of 500 kHz–20 mHz with a sinusoidal alternating voltage amplitude of 10 mV root-mean-square (rms). A cell equipped with two platinized platinum electrodes was utilized for conductivity measurements (TOA Electronics, CG-511B), and the cell constant was determined using a 0.01 M KCl aqueous solution at 25 °C. The cell was placed in a temperature-controlled chamber, and conductivity was measured at different temperatures with heating from 10–90 °C. The liquid density and viscosity were determined in the temperature range of 10–90 °C with a viscometer (Anton Paar, SVM 3000).

NMR spectroscopy was conducted to examine the dynamic coordination environment of the Na-based solvate IL. Pulsed-field gradient spin-echo (PGSE) NMR measurements were carried out to determine the self-diffusion coefficients of [Na(G5)_x][TFSA] ($x = 1$ and 2). A JEOL-ECX 400 NMR spectrometer with a 9.4 T narrow-bore super-conducting magnet equipped with a pulsed-field gradient probe and current amplifier was used for this purpose. Self-diffusion coefficients were calculated with the Hahn spin-echo sequence using ¹H from terminal methyl group of G5 and ¹⁹F from [TFSA]⁻ anion. The free diffusion echo signal attenuation E is related to the experimental parameters by the Stejskal equation with a sinusoidal pulsed-field gradient:²⁸

$$\ln(E) = \ln(S/S_{\delta=0}) = \frac{-\gamma^2 g^2 D \delta^2 (4\Delta - \delta)}{\pi^2}$$

where S is the spin-echo signal intensity, δ is the duration of the field gradient with magnitude g , γ is the gyromagnetic ratio and Δ is the interval between the two gradient pulses. The value of Δ was set at 50 ms. The sample was inserted into a NMR microtube to a height of 3 mm to exclude the convection. The measurements were conducted at 30 and 60 °C. ¹H NMR measurements for [Na(G5)_x][TFSA] ($x = 1$ and 2) and pure G5 were performed in order to measure the life-time of free glyme molecules in the mixture. The measurements were carried out using a JEOL-ECX 400 NMR spectrometer with a ¹H resonance frequency of 400 MHz at 30 °C. Each sample was placed in a sample tube with an outer diameter of 4 mm, and that tube was inserted into a 5

mm standard NMR sample tube. CDCl_3 for field/frequency lock and external standard was infused in the narrow space between the 4 and 5 mm tubes.

The electrochemical stabilities of $[\text{Na}(\text{G}5)_x][\text{TFSA}]$ ($x = 0.8, 1, \text{ and } 1.25$) were evaluated by linear sweep voltammetry (LSV) using an electrochemical analyzer (Princeton Applied Research, VMP3) and three-electrode cell with a scan rate of 1 mV s^{-1} . The working and counter electrodes were both platinum. The reference electrode was consisting of Li metal soaked in $[\text{Li}(\text{G}4)_1][\text{TFSA}]$, confined in a glass tube equipped with a liquid junction.

Charge-discharge characteristics of $[\text{Na}(\text{G}5)_x][\text{TFSA}]$ electrolyte ($x = 1 \text{ and } 1.25$) were tested using a 2032-type coin cell with a $[\text{Na anode} \mid [\text{Na}(\text{G}5)_x][\text{TFSA}] \text{ electrolyte} \mid \text{Na}_{0.44}\text{MnO}_2 \text{ cathode}]$. The composite cathode was prepared by thoroughly mixing $\text{Na}_{0.44}\text{MnO}_2$ as the cathode active material, acetylene black as an electrically conductive additive, and poly(vinylidene fluoride) as a binder in the a weight ratio of 80:10:10, respectively. The mixture was homogenized in a solvent of *N*-methylpyrrolidone to obtain a slurry. The slurry was pasted onto an aluminum current collector and dried at $80 \text{ }^\circ\text{C}$ for 12 h. The above obtained cathode sheet was compressed to improve the electrical conductivity and further dried under vacuum at $100 \text{ }^\circ\text{C}$ for 12 h before use. Sodium foil was used as an anode and a glass fiber filter (GA-55, ADVANTEC) was used as a separator. To ensure complete penetration of the electrolyte into the pressed cathode sheet, the fabricated cell was aged at $60 \text{ }^\circ\text{C}$ for 12 h. The charge–discharge test was carried out at $60 \text{ }^\circ\text{C}$ with a current density of $70 \text{ } \mu\text{A cm}^{-2}$ (12.15 mA g^{-1} based on the mass of $\text{Na}_{0.44}\text{MnO}_2$).

Calculations

Ab initio molecular orbital calculations were carried out using the Gaussian 03 program package.²⁹ The basis sets implemented in the Gaussian program were used. The geometries of G5 and $[\text{Na}(\text{G}5)_1][\text{TFSA}]$ were fully optimized at the HF/6-311G** level, and the HOMO energy levels were also calculated at the HF/6-311G** level. The atomic coordinates for initial geometries were obtained from the crystal structure of

[Na(G5)₁][TFSA] at -100 °C.²²

3. RESULTS AND DISCUSSION

3.1 Coordination Structure of [Na(G5)₁][TFSA]

Because the physicochemical properties such as electrochemical and transport properties are closely related to the speciation presented in solution, we first examined their coordination structures in solution. We have previously reported the phase diagrams of G5-Na[TFSA] binary mixtures, demonstrating that an equimolar mixture of them forms the relatively stable solvate [Na(G5)₁][TFSA] (melting point: 31.7 °C).²² Although the melting point of [Na(G5)₁][TFSA] is slightly higher than room temperature, it maintains its liquid state at 30 °C as a supercooled liquid. The single-crystal structure for [Na(G5)₁][TFSA] has also been clarified.²² In the crystal, the glyme (G5) wraps around the Na⁺ ion with a characteristic framework to form the complex cation [Na(G5)₁]⁺. The counter [TFSA]⁻ anions also coordinate to Na⁺ ions in a monodentate form, resulting in formation of a CIP-I (contact ion pair with a monodentate anion) type solvate. Raman analysis has verified that the 1:1 complex cation structure of [Na(G5)₁]⁺ is maintained even in the liquid state.²²

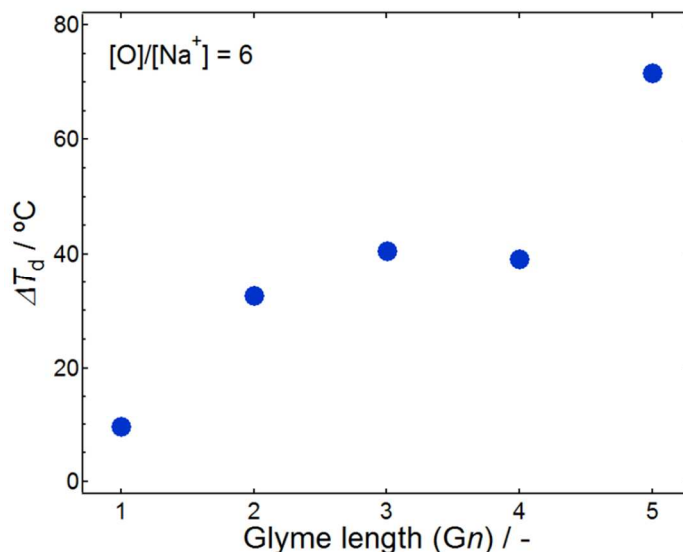


Figure 1. ΔT_d of glyme–Na[TFSA] mixtures at an [O]/[Na⁺] ratio of 6.

Based on the principles of coordination chemistry and solvate structure, glyme-Na[TFSA] binary mixtures with the ratio of Na^+ ions and oxygen atoms within solvents ($[\text{O}]/[\text{Na}^+]$) at 6 are likely to form stable complexes. As the strong ion-solvent interaction makes the complexes thermally stable,¹¹ TG measurements on a series of glyme-Na[TFSA] mixtures would be able to verify the interaction between Na^+ ions and different glyme ligands. **Figure 1** shows the difference in thermal decomposition temperatures (ΔT_d) between the pure solvents and mixtures having an $[\text{O}]/[\text{Na}^+]$ ratio of 6 ($[\text{Na}(\text{G1})_3][\text{TFSA}]$, $[\text{Na}(\text{G2})_2][\text{TFSA}]$, $[\text{Na}(\text{G3})_{1.5}][\text{TFSA}]$, $[\text{Na}(\text{G4})_{1.2}][\text{TFSA}]$, and $[\text{Na}(\text{G5})_1][\text{TFSA}]$), where T_d is defined as the temperature at 5% weight loss. The measured TG results are shown in **Figure S1** (Electronic Supplementary Information (ESI)). The substantially lower ΔT_d observed for $[\text{Na}(\text{G1})_3][\text{TFSA}]$ is attributed to the high volatility of the uncoordinating or weakly interacting solvents with Na^+ ions in the mixture. As increasing glyme length, the ΔT_d values of the mixtures became larger. The considerably high ΔT_d of $[\text{Na}(\text{G5})_1][\text{TFSA}]$ among all mixtures clearly demonstrates the strong ion-solvent interaction between the longer glyme (G5) and Na^+ ion. This structure-dependent interaction is ascribed to the chelate effect, which is well known to increase in strength as the number of coordination sites within a single ligand molecule is increased. The calculated structure also demonstrates the formation of a 1:1 complex. As shown in **Figure 2**, the optimized structure for $[\text{Na}(\text{G5})_1][\text{TFSA}]$ obtained by *ab initio* molecular orbital calculations, namely a CIP-I-type solvate composed of $[\text{Na}(\text{G5})_1]^+$ and $[\text{TFSA}]^-$ ions, is similar to the experimental structure.²²

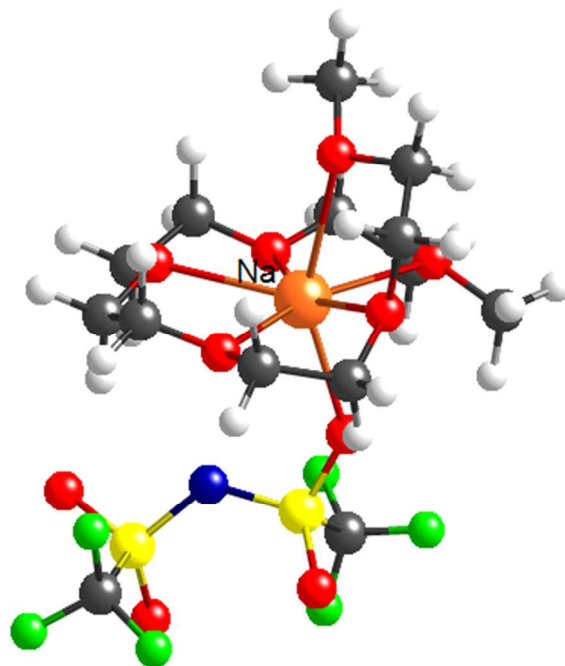


Figure 2. Optimized structure of $[\text{Na}(\text{G5})_1][\text{TFSA}]$ via *ab initio* molecular orbital calculations at the HF/6-311G** level. Orange, Na; red, O; gray, C; white, H; blue, N; yellow, S; green, F.

3.2 Transport Properties of G5-Na[TFSA] Binary Mixtures

Concentration effect. **Figure 3** shows the isothermal viscosity (η) and ionic conductivity (σ) of $[\text{Na}(\text{G5})_x][\text{TFSA}]$ at 30 °C as a function of Na[TFSA] molar concentration in solution. Molar concentration c was calculated from the solution density and molecular weight of Na[TFSA]. The viscosity of $[\text{Na}(\text{G5})_x][\text{TFSA}]$ was shown to increase drastically at concentrations higher than 2.5 mol dm⁻³. The molar concentration of molten solvate $[\text{Na}(\text{G5})_1][\text{TFSA}]$ was found to be approximately 2.5 mol dm⁻³ (**Table S1** in ESI), which is in good agreement with the concentration at which the abrupt increase in viscosity was observed. As concentration is increased, the population of the bulky complex cation of $[\text{Na}(\text{G5})_1]^+$ in the electrolyte is increased. In addition, the coulombic interaction between the complex cation and $[\text{TFSA}]^-$ anion would become stronger with an increase in concentration since the average distance between the cation and anion should decrease as concentration increases. This phenomenon causes the increase in mixture's viscosity.

The concentration dependent σ showed behavior typical to common electrolyte systems.³⁰⁻³³ The σ value

increased at first with an increase in molar concentration, reaching a maximum at around 1 mol dm^{-3} , whereas for a further concentrated system, the value decreased. The reason for this phenomenon can be explained in terms of the number and mobility of charge carriers. The number of charge carriers increases as concentration is increased. However, its mobility decreases simultaneously with increasing viscosity of the medium by adding Na[TFSA], as shown in **Figure 3**. These two effects compete mutually, resulting in the appearance of a σ maximum value.

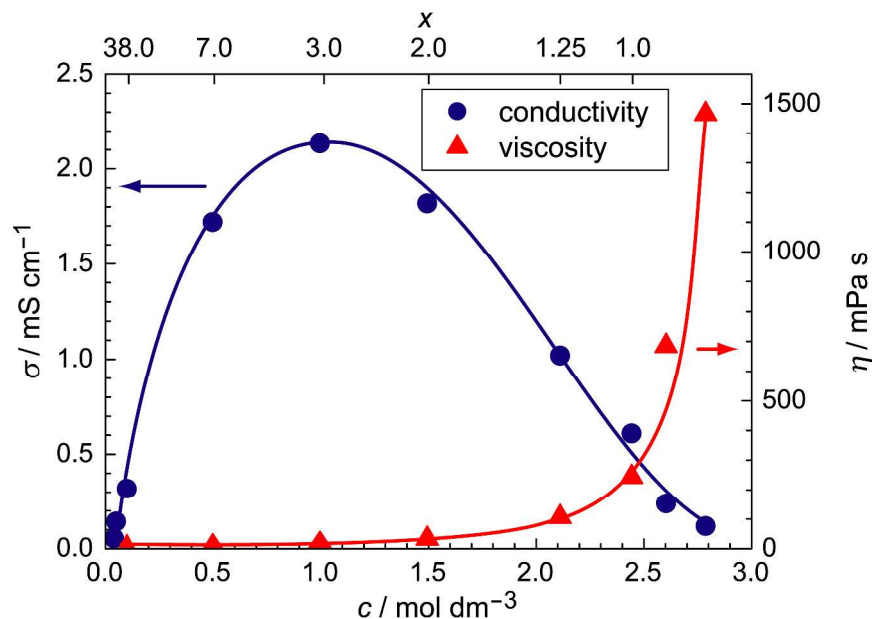


Figure 3. Concentration dependencies of viscosity (η) and ionic conductivity (σ) for the binary mixtures of Na[TFSA] and G5 at 30 °C; c is the molar concentration of Na[TFSA], and x is the molar ratio of Na[TFSA] and G5 in $[\text{Na}(\text{G5})_x][\text{TFSA}]$. The lines in the figure function as guidelines for the eye.

The diffusion coefficient of each species in the complex is very helpful in discussing the coordination state of the complex. Nevertheless, measuring the diffusion coefficient of Na^+ ions by PGSE-NMR spectroscopy is extremely difficult due to the intrinsic chemical nature of the Na nucleus. Instead, we can measure the diffusion coefficients of glymes and paired anions because of the involvement of NMR-sensitive ^1H and ^{19}F nuclei in G5 and the $[\text{TFSA}]^-$ anion, respectively. **Table 1** shows the diffusion coefficients of G5 and $[\text{TFSA}]^-$ of $[\text{Na}(\text{G5})_1][\text{TFSA}]$ and $[\text{Na}(\text{G5})_2][\text{TFSA}]$. As reported previously, G5 molecules coordinate to Na^+ ions in a 1:1

molar ratio to form the complex cation of $[\text{Na}(\text{G5})_1]^+$ in the liquid state, similar to that in the crystalline state.²² Thus, we can assume that the coordinating G5 molecule and Na^+ ion diffuse together in the liquid $[\text{Na}(\text{G5})_1][\text{TFSA}]$, consequently, the diffusion rate of Na^+ ion corresponds to that of G5. For $[\text{Na}(\text{G5})_1][\text{TFSA}]$, the diffusion coefficients of G5 and $[\text{TFSA}]^-$ anion showed an almost identical value, but with $[\text{TFSA}]^-$ diffusing slightly faster than G5. As listed in **Table 1** (D_{glyme}/D_-), this minute difference became more evident with increasing temperature, suggesting that $[\text{Na}(\text{G5})_1]^+$ cations and $[\text{TFSA}]^-$ anions are partially dissociated in the liquid state. As evidenced by their Raman spectra, however, they are present predominantly as CIPs in the liquid state.²² This discrepancy can be understood by the ion-exchange reaction, i.e., dynamic coordination exchange, between the $[\text{Na}(\text{G5})_1]^+$ cation and $[\text{TFSA}]^-$ anion.

In contrast, the diffusion coefficient of G5 in $[\text{Na}(\text{G5})_2][\text{TFSA}]$ was larger than that of the $[\text{TFSA}]^-$ anion. Two types of G5 are expected in $[\text{Na}(\text{G5})_2][\text{TFSA}]$, one in which is G5 coordinating to the Na^+ ion and the other is the uncoordinating (or free) G5. Raman spectrum has also proven this assumption.²² Because these two glymes could not be distinguished by NMR spectroscopy due to ligand exchange of the complex $[\text{Na}(\text{G5})_1]^+$ cation ($[\text{Na}(\text{G5})_1]^+ + \text{G5}^* \rightleftharpoons [\text{Na}(\text{G5}^*)_1]^+ + \text{G5}$), the measured diffusion coefficients presented are the average values of these types. The D_{glyme}/D_- ratio in $[\text{Na}(\text{G5})_2][\text{TFSA}]$ was found to be larger than that in $[\text{Na}(\text{G5})_1][\text{TFSA}]$, suggesting that the uncoordinating glyme molecules diffuse faster than the coordinating ones.

Table 1. Diffusion coefficients of G5 (glyme) and $[\text{TFSA}]^-$ anions at 30 and 60 °C.

Sample	$T / ^\circ\text{C}$	Diffusion coefficient / $10^{-7} \text{ cm}^2 \text{ s}^{-1}$		D_{glyme}/D_-
		D_{glyme}	D_-	
$[\text{Na}(\text{G5})_1][\text{TFSA}]$	30	0.44	0.45	0.98
$[\text{Na}(\text{G5})_2][\text{TFSA}]$	30	2.61	2.18	1.20
$[\text{Na}(\text{G5})_1][\text{TFSA}]$	60	2.60	2.67	0.97
$[\text{Na}(\text{G5})_2][\text{TFSA}]$	60	10.24	9.39	1.09

Investigation of the ligand exchange rate of the complex $[\text{Na}(\text{G5})_1]^+$ cation in the liquid is also of interest to this study. To evaluate the ligand exchange rate in the mixtures, ^1H NMR spectra of pure G5 and $[\text{Na}(\text{G5})_x][\text{TFSA}]$ ($x = 1$ and 2) were obtained as shown in **Figure S2** (ESI). When one-half of the G5 molecules coordinate with Na^+ ions in the $[\text{Na}(\text{G5})_2][\text{TFSA}]$ mixture and ligand exchange takes place, the exchange rate (k_{ex}) can be expressed as follows:^{34, 35}

$$k_{\text{ex}} = \frac{\pi(\delta\nu)^2}{(W - W_0)}$$

where W_0 and W are the full width at half-maximum (fwhm) of the NMR signal of the terminal methyl protons of pure G5 and $[\text{Na}(\text{G5})_2][\text{TFSA}]$, respectively. The $\delta\nu$ is the difference in chemical shift of the end methyl protons of $[\text{Na}(\text{G5})_1][\text{TFSA}]$ and pure G5. $[\text{Na}(\text{G5})_2][\text{TFSA}]$ is assumed to be a mixture of $[\text{Na}(\text{G5})_1][\text{TFSA}]$ and excess G5. By using this equation, k_{ex} in $[\text{Na}(\text{G5})_2][\text{TFSA}]$ ($c = 1.5 \text{ mol dm}^{-3}$) was estimated as $9.6 \times 10^3 \text{ s}^{-1}$, and the life-time ($\tau = 1/k_{\text{ex}}$) of complex $[\text{Na}(\text{G5})_1]^+$ cation in the liquid was estimated as $1.0 \times 10^{-4} \text{ s}$. This life-time of $[\text{Na}(\text{G5})_1]^+$ cation is much longer than that of $[\text{Na}(\text{H}_2\text{O})_x]^+$ consisting of a monodentate ligand (H_2O) in aqueous solutions ($\tau < 10^{-8} \text{ s}$).³⁶ The ligand exchange rate can thus be estimated for the excess-glyme containing solution of $[\text{Na}(\text{G5})_2][\text{TFSA}]$, and the exchange rate should become slower (the life-time of the complex $[\text{Na}(\text{G5})_1]^+$ cation should become longer while the life-time of free G5 should become shorter) as the molar ratio of G5 decreases in the liquid. It is presumable that a Na^+ ion and G5 molecule form a long-lived complex $[\text{Na}(\text{G5})_1]^+$ cation ($\tau > 10^{-4} \text{ s}$) in the equimolar molten $[\text{Na}(\text{G5})_1][\text{TFSA}]$ complex because free glymes scarcely exist in the molten complex. These results support the view that molten $[\text{Na}(\text{G5})_1][\text{TFSA}]$ is composed of a solvate $[\text{Na}(\text{G5})_1]^+$ cation and $[\text{TFSA}]^-$ anion and can thus be categorized as a solvate IL.

It is noteworthy that the ligand exchange rates for $[\text{Li}(\text{G3})_2][\text{TFSA}]$ and $[\text{Li}(\text{G4})_2][\text{TFSA}]$ were 5.2×10^3 and $2.8 \times 10^3 \text{ s}^{-1}$, respectively.¹² Regardless of the longer ligand, the ligand exchange rate for $[\text{Na}(\text{G5})_2][\text{TFSA}]$ was slightly higher than those of glyme-Li systems. The electric field of the Na^+ ion is weaker than that of Li^+ ion

because of its larger radius. This causes a weaker ion-dipole interaction between Na^+ and glyme, resulting in the relatively high rate of ligand exchange.

To gain deeper insight into the ionic nature of the concentrated system, ionicity of the system was evaluated. Ionicity, or the ratio of molar conductivity ($A_{\text{imp}}/A_{\text{NMR}}$), has been previously used to estimate the degree of dissociation of lithium salts in dilute electrolytes,^{37,38} and can also be a useful metric for quantifying the dissociativity or degree of correlative motion of the ions, even in extremely concentrated systems such as ILs.^{39–42} Ionicity is defined as the molar conductivity ratio, $A_{\text{imp}}/A_{\text{NMR}}$, where A_{imp} and A_{NMR} are the molar conductivities obtained from electrochemical impedance measurements and PGSE-NMR spectroscopy, respectively. This can be written as follows:

$$A_{\text{imp}} = \frac{\sigma}{c}$$

$$A_{\text{NMR}} = \frac{F^2}{RT} (D_+ + D_-)$$

where F is the Faraday constant, R is the gas constant, T is the absolute temperature, and D_+ and D_- are the self-diffusion coefficients of cation and anion obtained from PGSE-NMR, respectively. This equation assumes that all diffusing species detected by PGSE-NMR contribute to the molar conductivity. Ionicity values for typical aprotic and protic ILs have been widely studied, and have been found to be comparable to traditional electrolyte solutions.¹⁴ Glyme-Li salt mixtures with different concentrations and anionic structures have also been systematically investigated.^{11,14} The ionicity values for $[\text{Li}(\text{G}3)_1][\text{TFSA}]$ and $[\text{Li}(\text{G}4)_1][\text{TFSA}]$, representative solvate ILs, are 0.68 and 0.63 at 30 °C, respectively.¹¹

Unfortunately, a valid A_{NMR} value for $[\text{Na}(\text{G}5)_x][\text{TFSA}]$ cannot be collected as stated before. The above assumption used for estimating the ligand exchange rate is available only for $[\text{Na}(\text{G}5)_1][\text{TSFA}]$. For these systems, $A_{\text{imp}}/A_{\text{ideal}}$ would be effective as an alternative indicator of ionicity.⁴³ The product of molar conductivity A_{imp} and η becomes constant if the solution obeys Walden's rule. The Walden plot ($\log A$ versus $\log(1/\eta)$) of a 1.0 M aqueous KCl solution where K^+ cation and Cl^- anion are totally dissociated is considered to be an ideal

straight line with a slope of unity. From the ideal line, a A_{ideal} value at certain η can be expected. Previous investigations of the relationship between $A_{\text{imp}}/A_{\text{NMR}}$ and $A_{\text{imp}}/A_{\text{ideal}}$ of ILs and equimolar glyme-Li salt mixtures have shown a decent consistency.^{14, 44}

Figure 4 shows the concentration dependency of ionicity ($A_{\text{imp}}/A_{\text{ideal}}$) for $[\text{Na}(\text{G5})_x][\text{TFSA}]$ at 30 °C. $[\text{Na}(\text{G5})_1][\text{TFSA}]$ was observed to have an ionicity value of 0.63, comparable to $[\text{Li}(\text{glyme})_1][\text{TFSA}]$ systems. As shown in **Figure 4**, its ionicity became larger with increasing concentration in the range of 0.01–2.5 mol dm^{-3} . This result is similar to our previous results observed in not only binary glyme-Li[TFSA] mixtures,^{11,14} but also in aprotic IL/solvent mixtures,³⁹ indicating that $[\text{Na}(\text{G5})_1][\text{TFSA}]$ behaves similarly to $[\text{Li}(\text{glyme})_1][\text{TFSA}]$ as well as aprotic ILs. This type of behavior is opposite to that observed in conventional organic electrolyte solutions consisting of alkali metal salts and polar solvents.⁴⁵ Although the precise explanation for these opposing phenomena accompanying an increment in concentration cannot be made, it may be interpreted by a nano-inhomogeneity of the mixtures. For aprotic IL/solvent mixtures, the presence of an ionic cluster is suggested in the case of incorporating low-polar solvents.^{46–49} Actually, glymes are low-polar solvents. The relative permittivity (ϵ_r) values of G1–G4 at ambient temperature are in the range of 7.2–7.7,^{50,51} therefore, the ϵ_r of G5 is also expected to be 7–8. This value is substantially low compared to those of polar solvents, such as propylene carbonate ($\epsilon_r = 65$) and dimethyl sulfoxide ($\epsilon_r = 46.5$),⁵² which are often used as solvents for conventional organic electrolytes. Low-polar solvents serve as low dielectric media. The electrostatic force between cation and anion increases as decreasing the relative permittivity of solvent in electrolyte solution. Thus, interionic attractive forces would be enhanced in the presence of low-polar solvents, rather than in neat ILs with well-balanced ionic interactions. This situation causes formation of ionic clusters in the IL/low-polar solvent mixtures, resulting in low ionicity. The excess glyme containing $[\text{Na}(\text{G5})_x][\text{TFSA}]$ ($x > 1$) can be regarded as a mixture of $[\text{Na}(\text{G5})_1][\text{TFSA}]/(x-1)\text{G5}$, and hence, the diluted solutions appear comparable to aprotic IL/low-polar solvent systems. Therefore, ionic cluster formation induced by the presence

of excess glyme molecules may account for the anomalous behavior in the concentration dependent ionicity of $[\text{Na}(\text{G5})_x][\text{TFSA}]$. It should be noted that, at very low salt concentration ($< 3 \text{ mM}$), the ionicity increases again with decreasing the salt concentration as predicted by classical electrolyte theories (**Figure S3** and **Table S1**).^{52–54} This result indicates that ion-pairs dissociate into their constituent ions at extremely low concentration even in a low-polar medium. The Walden plot (**Figure S4**) also clearly reflects a variation of the ionic state depending on the concentration.

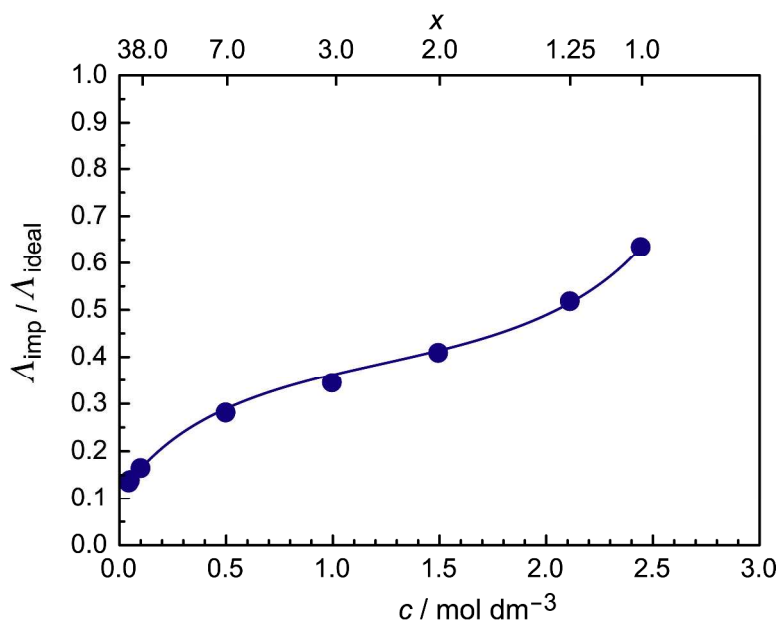


Figure 4. Ionicity ($A_{\text{imp}}/A_{\text{ideal}}$) of $[\text{Na}(\text{G5})_x][\text{TFSA}]$ as a function of concentration at 30 °C. The line in the figure functions as a guideline for the eye.

Temperature effect: The temperature dependencies of η and σ for $[\text{Na}(\text{G5})_1][\text{TFSA}]$ are shown in **Figure 5** in the form of an Arrhenius plot. The σ values appeared to increase with elevating temperature and showed convex-curved profiles as described by the following Vogel-Tamman-Fulcher (VTF) equation:

$$\sigma = \sigma_0 \exp \left[\frac{-B}{T - T_0} \right]$$

where σ_0 , B , and T_0 are constants. The best fit values for each parameter were $\sigma_0 = 4.71 \times 10^{-1} \text{ S cm}^{-1}$, $B = 6.69 \times 10^2 \text{ K}$, and $T_0 = 202 \text{ K}$. Among the obtained values, T_0 for $[\text{Na}(\text{G5})_1][\text{TFSA}]$ was higher compared to that

for $[\text{Li}(\text{G3})_1][\text{TFSA}]$.¹¹ In contrast, temperature dependent η decreased with elevating temperature, showing a concave-curved profile as described by the following VTF equation:

$$\eta = \eta_0 \exp \left[\frac{B}{T - T_0} \right]$$

where η_0 , B , and T_0 are constants. The best fit values for each parameter were $\eta_0 = 5.1 \times 10^{-2}$ mPa s, $B = 9.96 \times 10^2$ K, and $T_0 = 185$ K. Similar to the VTF parameters in the temperature dependent σ , the T_0 value for $[\text{Na}(\text{G5})_1][\text{TFSA}]$ was higher than that for $[\text{Li}(\text{G3})_1][\text{TFSA}]$.¹¹ These higher T_0 parameters observed for both σ and η suggest a stronger cohesive energy of $[\text{Na}(\text{G5})_1][\text{TFSA}]$ than that of $[\text{Li}(\text{G3})_1][\text{TFSA}]$.

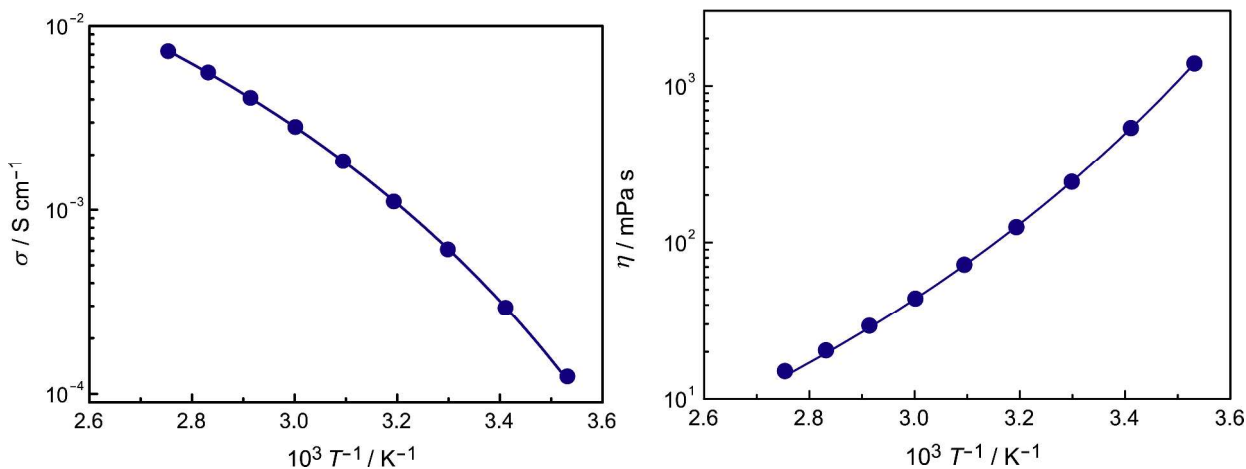


Figure 5. Arrhenius plots of ionic conductivity (left) and viscosity (right) for $[\text{Na}(\text{G5})_1][\text{TFSA}]$.

The temperature dependency of liquid density (ρ) for $[\text{Na}(\text{G5})_1][\text{TFSA}]$ is depicted in **Figure 6**. The density decreases linearly with elevating temperature and can be expressed by the following equation:

$$\rho = b - aT$$

where T is the absolute temperature (K), and a and b are constants with values of $a = 1.0 \times 10^{-3}$ g cm⁻³ K⁻¹ and $b = 1.695$ g cm⁻³.

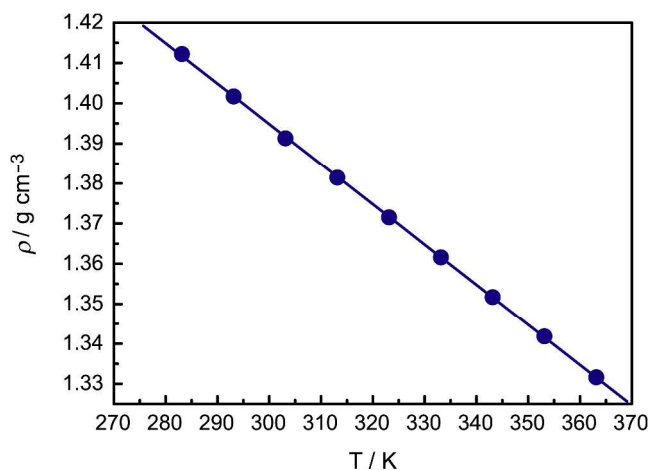


Figure 6. Temperature dependence of liquid density for $[\text{Na}(\text{G5})_1][\text{TFSA}]$.

As reported previously, $[\text{Na}(\text{G5})_1][\text{TFSA}]$ exhibited an exceptionally higher thermal stability compared to its diluted solutions since the equimolar mixture of $\text{Na}[\text{TFSA}]$ and G5 forms a long-lived complex cation, $[\text{Na}(\text{G5})_1]^+$, even at 150 °C.²² This remarkable thermal stability is favorable for the use of $[\text{Na}(\text{G5})_1][\text{TFSA}]$ as a highly safe electrolyte for Na secondary batteries instead of conventional organic electrolytes. The electrochemical properties and battery performance of the $[\text{Na}(\text{G5})_x][\text{TFSA}]$ electrolyte are discussed in the next section.

3.3 Electrochemical Properties and Battery Application

The oxidative stabilities of the G5-Na[TFSA] binary mixtures were investigated by linear sweep voltammetry (LSV) at 30 and 60 °C. **Figure 7** shows the LSV results of $[\text{Na}(\text{G5})_x][\text{TFSA}]$ ($x = 0.8, 1, \text{ and } 1.25$). In these systems, a sharp rise in anodic current is known to result from the oxidation of glymes. **Figure 7** clearly illustrates that the oxidative stability became higher with increasing concentration irrespective of operating temperature. In addition, a comparison of stabilities for each mixture with the same concentration at different temperatures revealed that the elevated temperature leads to lower stability in the mixtures.

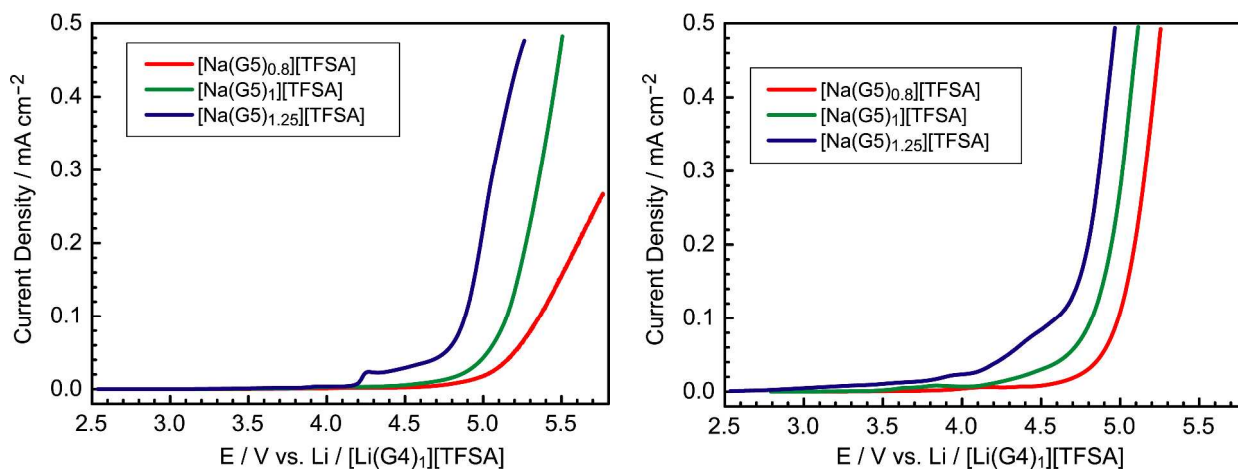


Figure 7. LSV curves for $[\text{Na}(\text{G5})_x][\text{TFSA}]$ ($x = 0.8, 1, 1.25$) at 30 (left) and 60 (right) °C.

To discuss the oxidative stability of the complexes in further detail, variations in the HOMO energy levels through complexation were evaluated by *ab initio* molecular orbital calculations based on the optimized structure shown in **Figure 2**. The calculated HOMO energy levels for G5 (all *trans* conformation), $[\text{Na}(\text{G5})_1]^+$, and $[\text{Na}(\text{G5})_1][\text{TFSA}]$ are listed in **Table 2**. The electrochemical oxidation of glyme molecules at the electrode/electrolyte interface occurs when electrons are extracted from the HOMO of glyme. Thus, the lower HOMO energy level leads to a higher oxidative stability. From the calculated result, the HOMO energy level of $[\text{Na}(\text{G5})_1]^+$ appeared lower than that of G5, indicating that the HOMO energy level of G5 is lowered by complexation. When G5 and Na^+ ion form a complex cation, the G5 molecule is highly polarized by the strong electric field of Na^+ ion which serves to stabilize the orbitals of ether oxygen atoms containing lone-pair electrons, resulting in the lowering of its HOMO energy level. The HOMO energy level of $[\text{Na}(\text{G5})_1][\text{TFSA}]$ appeared higher than that of $[\text{Na}(\text{G5})_1]^+$ because of a weakening of the Na^+ cation electric field by the negatively charged $[\text{TFSA}]^-$ anion, however, the HOMO energy level of $[\text{Na}(\text{G5})_1][\text{TFSA}]$ was still lower than that of pure G5. A similar result has also been reported for $[\text{Li}(\text{glyme})_1][\text{TFSA}]$.^{12,55} As shown in **Figure 7**, as the molar ratio of G5 in the electrolyte was decreased, the oxidative stability was improved. In the case of $[\text{Na}(\text{G5})_{1.25}][\text{TFSA}]$, certain amounts of uncoordinating free G5 are present in the mixture. This free G5 can be

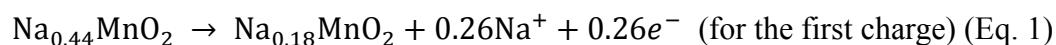
oxidized at a lower electrode potential than the coordinating G5. On the other hand, free glyme molecules are scarce in the equimolar complex of $[\text{Na}(\text{G5})_1][\text{TFSA}]$, leading to its higher oxidative stability. Although the calculation of HOMO energy levels is based on the coordination structure in the crystalline state, the calculations suitably account for the improvement in oxidative stability of glyme by complex formation, suggesting that the complex structures of $[\text{Na}(\text{G5})_1]^+$ and $[\text{Na}(\text{G5})_1][\text{TFSA}]$ are retained to a great extent even in the liquid state. This is also supported by the comparison of Raman spectra between solid- and liquid-state $[\text{Na}(\text{G5})_1][\text{TFSA}]$.²²

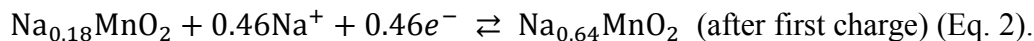
Table 2. HOMO energy levels of glymes calculated by HF/6-311G** level *ab initio* molecular orbital calculations.

Sample	Atomic unit	eV	ΔeV^a
G5 (all trans)	-0.42133	-11.46	0
$[\text{Na}(\text{G5})_1]^+$	-0.54421	-14.81	-3.35
$[\text{Na}(\text{G5})_1][\text{TFSA}]$	-0.44036	-11.98	-0.52

^a ΔeV is the change in the HOMO level associated with complex formation from that of the isolated *all trans* G5.

From the LSV result, $[\text{Na}(\text{G5})_1][\text{TFSA}]$ showed a decent oxidative stability below 4.5 V, indicating its possible use as a liquid electrolyte for Na-ion batteries with 4 V class cathodes. To examine the possibility of $[\text{Na}(\text{G5})_1][\text{TFSA}]$ as an electrolyte for batteries, the battery tests were carried out. **Figure 8a** shows the galvanostatic charge–discharge curves of a $[\text{Na metal} | [\text{Na}(\text{G5})_1][\text{TFSA}] | \text{Na}_{0.44}\text{MnO}_2]$ cell operated at 60 °C. As the temperature was increased from 30 to 60 °C, the viscosity and ionic conductivity of $[\text{Na}(\text{G5})_1][\text{TFSA}]$ were greatly decreased and increased, respectively (**Table S2** in ESI), resulting in the lowering of internal cell resistance. The cell showed reversible charge–discharge behavior with a capacity of about 110 mA h g⁻¹ in the first 10 cycles except for the first charge. Through this charge–discharge process, Na⁺ ions are reversibly extracted/inserted from/into the framework structure constructed of MnO₂ with a varying composition of cathode active material, as follows:²⁷





As described in Eq. 1, the amount of Na^+ ions deintercalated from $\text{Na}_{0.44}\text{MnO}_2$ are lower for the first charge process compared to those after first charge, resulting in the exceptionally low charge capacity at the first charge process. The charge–discharge coulombic efficiency was approximately 90% at the second cycle. The efficiency improved with increasing cycle number, reaching over 95% after 30 cycles (**Figure 9**). Although the capacity gradually decreased through cycling, the cell with $[\text{Na}(\text{G5})_1][\text{TFSA}]$ exhibited highly reversible charge–discharge behavior. The charge–discharge test performed at 30 °C at a low current density of $10 \mu\text{A cm}^{-2}$ (2.94 mA g^{-1} based on the mass of $\text{Na}_{0.44}\text{MnO}_2$) also verified the good reversibility of this cell (**Figure S5**).

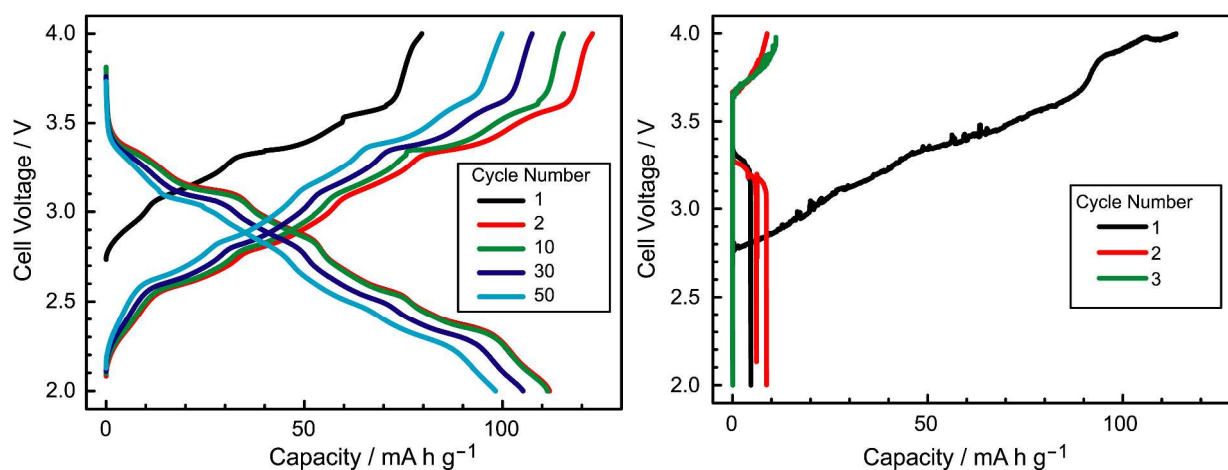


Figure 8. Charge–discharge curves of $[\text{Na} | [\text{Na}(\text{G5})_1][\text{TFSA}] | \text{Na}_{0.44}\text{MnO}_2]$ (a) and $[\text{Na} | [\text{Na}(\text{G5})_{1.25}][\text{TFSA}] | \text{Na}_{0.44}\text{MnO}_2]$ (b) at 60 °C.

In contrast, in the case of $[\text{Na}(\text{G5})_x][\text{TFSA}]$ ($x > 1$) electrolytes, the battery cycle performances changed drastically as shown in **Figure 8b**. At the first charge process, a large irreversible capacity was observed, after which the cell could no longer charge and discharge. This observation is presumed to arise from the oxidative stability of the electrolyte. An oxidation current due to the oxidation of uncoordinating excess glyme was detected at ca. 3.0 V in the LSV curve for $[\text{Na}(\text{G5})_{1.25}][\text{TFSA}]$ at 60 °C, while $[\text{Na}(\text{G5})_1][\text{TFSA}]$ and $[\text{Na}(\text{G5})_{0.8}][\text{TFSA}]$, having no excess glyme molecules, possessed higher oxidative stabilities (**Figure 7**).

Because the battery test was performed in the voltage range of 2.0–4.0 V, the uncoordinating glymes were oxidatively decomposed at the cathode surface. The electrode surface would therefore be covered by the decomposition products after the first charge, preventing further proper electrochemical reactions from occurring. Thus, it can be concluded that the undesired reaction originating from the oxidation of excess glymes causes the unsuccessful charge–discharge of the $[\text{Na} \mid [\text{Na}(\text{G}5)_{1.25}][\text{TFSA}] \mid \text{Na}_{0.44}\text{MnO}_2]$ cell. Furthermore, these results also clearly indicate that the presence or absence of free glymes in the electrolyte has a significant impact on battery performance.

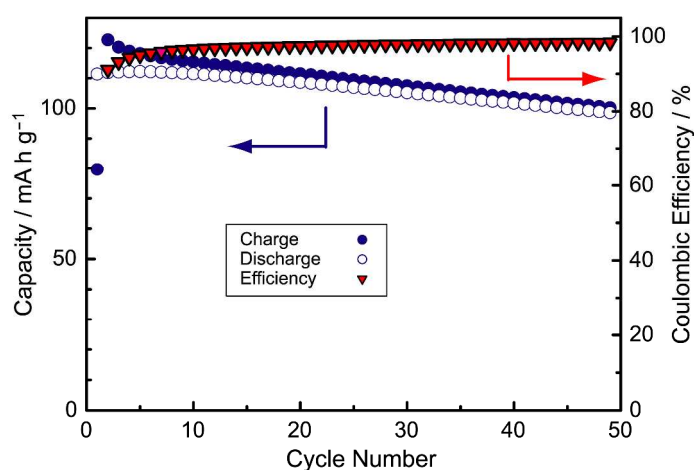


Figure 9. Charge–discharge capacities and coulombic efficiency of $[\text{Na} \mid [\text{Na}(\text{G}5)_1][\text{TFSA}] \mid \text{Na}_{0.44}\text{MnO}_2]$.

4. CONCLUSIONS

The physicochemical properties of a series of G5-Na[TFSA] binary mixtures were explored. The equimolar mixture of G5 and Na[TFSA] forms a low melting solvate. Lone pairs of electrons on oxygen atoms for the glyme (G5) are attracted to the Na^+ ions through ion-dipole interaction, and the glyme molecule wraps around the Na^+ ion to form a complex $[\text{Na}(\text{G}5)_1]^+$ cation. The ligand exchange rate of $[\text{Na}(\text{G}5)_1]^+$ in the G5-Na[TFSA] binary mixture was investigated using NMR, revealing that the G5 and Na^+ form a long-lived complex cation ($[\text{Na}(\text{G}5)_1]^+$) with a life time $> 10^{-4}$ s in concentrated mixtures ($c > 1.5 \text{ mol dm}^{-3}$). The molten solvate of $[\text{Na}(\text{G}5)_1][\text{TFSA}]$ exhibited an ionic conductivity of 0.61 mS cm^{-1} at $30 \text{ }^\circ\text{C}$, suggesting that $[\text{Na}(\text{G}5)_1][\text{TFSA}]$

dissociates into $[\text{Na}(\text{G5})_1]^+$ cation and $[\text{TFSA}]^-$ anion in the liquid. The ionicity ($A_{\text{imp}}/A_{\text{ideal}}$) of $[\text{Na}(\text{G5})_1][\text{TFSA}]$ was as high as 0.63 at 30 °C, regardless of extreme solution concentrations, which also supports the ionic nature of the molten complex.

The electrochemical properties of $[\text{Na}(\text{G5})_x][\text{TFSA}]$ as electrolytes for Na secondary batteries were also investigated. LSV experiments revealed that the oxidative stability of G5-Na[TFSA] mixtures increased with an increasing concentration of Na[TFSA]. This result was clearly interpreted from the variation in the HOMO energy level of G5 through the formation of $[\text{Na}(\text{G5})_1]^+$ complexes and $[\text{Na}(\text{G5})_1][\text{TFSA}]$ in the liquid, as evidenced by quantum chemical calculations. The improved oxidative stability of electrolytes due to complexation enabled the stable charge and discharge of a Na cell of $[\text{Na} | [\text{Na}(\text{G5})_1][\text{TFSA}] | \text{Na}_{0.44}\text{MnO}_2]$ in the voltage range of 2.0–4.0 V. The cell containing $[\text{Na}(\text{G5})_1][\text{TFSA}]$ showed a good cycle stability with a capacity of ca. 100 mA h g⁻¹ for 50 cycles, while the cell consisting of $[\text{Na}(\text{G5})_x][\text{TFSA}]$ ($x > 1$) with excess glyme could not be operated. According to these results, applying $[\text{Na}(\text{G5})_1][\text{TFSA}]$ as an electrolyte will make it possible to fabricate the safe Na secondary batteries that operate at ambient conditions.

Acknowledgements

This study was supported in part by the Advanced Low Carbon Technology Research and Development Program (ALCA) of the Japan Science and Technology Agency (JST), the Technology Research Grant Program of the New Energy and Industrial Technology Development Organization (NEDO) of Japan, and the MEXT program “Elements Strategy Initiative to Form Core Research Center”, Ministry of Education Culture, Sports, Science and Technology (MEXT) of Japan.

REFERENCES

1. B. L. Ellis, L. F. Nazar, *Curr. Opin. Solid St. M.*, 2012, **16**, 168–177.
2. A. Yaksic, J. E. Tilton, *Resources Policy*, 2009, **34**, 185–194.
3. T. Oshima, M. Kajita, A. Okuno, *Int. J. Appl. Ceram. Tec.*, 2004, **1**, 269–276.
4. N. Yabuuchi, M. Kajiyama, J. Iwatate, H. Nishikawa, S. Hitomi, R. Okuyama, R. Usui, Y. Yamada, S. Komaba, *Nat. Mater.*, 2012, **11**, 512–517.
5. S. Komaba, W. Murata, T. Ishikawa, N. Yabuuchi, T. Ozeki, T. Nakayama, A. Ogata, K. Gotoh, K. Fujiwara, *Adv. Funct. Mater.*, 2011, **21**, 3859–3867.
6. C. Delmas, J.-J. Braconnier, C. Fouassier, P. Hagenmuller, *Solid State Ionics*, 1981, **3–4**, 165–169.
7. H. Pan, Y.-S. Hu, L. Chen, *Energy Environ. Sci.*, 2013, **6**, 2338–2360.
8. J.-M. Tarascon, G. W. Hill, *Solid State Ionics*, 1986, **22**, 85–96.
9. W. A. Henderson, F. McKenna, M. A. Khan, N. R. Brooks, V. G. Young, Jr., R. Frech, *Chem. Mater.*, 2005, **17**, 2284–2289.
10. W. A. Henderson, N. R. Brooks, W. W. Brennessel, V. G. Young, Jr., *Chem. Matter.*, 2003, **15**, 4679–4684.
11. K. Yoshida, M. Tsuchiya, N. Tachikawa, K. Dokko, M. Watanabe, *J. Phys. Chem. C*, 2011, **115**, 18384–18394.
12. K. Yoshida, M. Nakamura, Y. Kazue, N. Tachikawa, S. Tsuzuki, S. Seki, K. Dokko, M. Watanabe, *J. Am. Chem. Soc.*, 2011, **133**, 13121–13129.
13. T. Tamura, K. Yoshida, T. Hachida, M. Tsuchiya, M. Nakamura, Y. Kazue, N. Tachikawa, K. Dokko, M. Watanabe, *Chem. Lett.*, 2010, **39**, 753–755.
14. K. Ueno, K. Yoshida, M. Tsuchiya, N. Tachikawa, K. Dokko, M. Watanabe, *J. Phys. Chem. B*, 2012, **116**, 11323–11331.
15. C. A. Angell, Y. Ansari, Z. Zhao, *Faraday Discuss.*, 2012, **154**, 9–27.

16. S. Seki, K. Takei, H. Miyashiro, M. Watanabe, *J. Electrochem. Soc.*, 2011, **158**, A769–A774.
17. A. Orita, K. Kamijima, M. Yoshida, K. Dokko, M. Watanabe, *J Power Sources*, 2011, **196**, 3874–3880.
18. K. Yoshida, M. Tsuchiya, N. Tachikawa, K. Dokko, M. Watanabe, *J. Electrochem. Soc.*, 2012, **159**, A1005–A1012.
19. N. Tachikawa, K. Yamauchi, E. Takashima, J.-W. Park, K. Dokko, M. Watanabe, *Chem. Commun.*, 2011, **47**, 8157–8159.
20. K. Dokko, N. Tachikawa, K. Yamauchi, M. Tsuchiya, A. Yamazaki, E. Takashima, J.-W. Park, K. Ueno, S. Seki, N. Serizawa, M. Watanabe, *J. Electrochem. Soc.*, 2013, **160**, A1304–A1310.
21. K. Ueno, J.-W. Park, A. Yamazaki, T. Mandai, N. Tachikawa, K. Dokko, M. Watanabe, *J. Phys. Chem. C*, 2013, **117**, 20509–20516.
22. T. Mandai, N. Nozawa, S. Tsuzuki, K. Yoshida, K. Ueno, K. Dokko, M. Watanabe, *J. Phys. Chem. B*, 2013, **117**, 15072–15085.
23. D. Monti, E. Jonsson, M. R. Palacin, P. Johansson, *J. Power Sources*, 2014, **245**, 630–636.
24. N. Wongittharom, T.-C. Lee, C.-H. Wang, Y.-C. Wang, J.-K. Chang, *J. Mater. Chem. A*, 2014, **2**, 5655–5661.
25. R. Hagiwara, K. Tamaki, K. Kubota, T. Goto, T. Nohira, *J. Chem. Eng. Data*, 2008, **53**, 355–358.
26. F. Sauvage, E. Baudrin, J.-M. Tarascon, *Sensor. Actuat. B-Chem*, 2007, **120**, 638–644.
27. F. Sauvage, L. Laffont, J.-M. Tarascon, E. Baudrin, *Inorg. Chem.*, 2007, **46**, 3289–3294.
28. E. O. Stejskal, J. E. Tanner, *J. Chem. Phys.*, 1965, **42**, 288–292.
29. M. J. Frisch, G. W. Trucks, H. B. Schlegel, G. E. Scuseria, M. A. Robb, J. R. Cheeseman, J. A. Montgomery, Jr., T. Vreven, K. N. Kudin, J. C. Burant, J. M. Millam, S. S. Iyengar, J. Tomasi, V. Barone, B. Mennucci, M. Cossi, G. Scalmani, N. Rega, G. A. Petersson, H. Nakatsuji, M. Hada, M. Ehara, K. Toyota, R. Fukuda, J. Hasegawa, M. Ishida, T. Nakajima, Y. Honda, O. Kitao, H. Nakai, M. Klene, X. Li, J. E. Knox, H. P. Hratchian, J. B. Cross, V. Bakken, C. Adamo, J. Jaramillo, R. Gomperts, R. E. Stratmann, O. Yazyev, A. J.

- Austin, R. Cammi, C. Pomelli, J. W. Ochterski, P. Y. Ayala, K. Morokuma, G. A. Voth, P. Salvador, J. J. Dannenberg, V. G. Zakrzewski, S. Dapprich, A. D. Daniels, M. C. Strain, O. Farkas, D. K. Malick, A. D. Rabuck, K. Raghavachari, J. B. Foresman, J. V. Ortiz, Q. Cui, A. G. Baboul, S. Clifford, J. Cioslowski, B. B. Stefanov, G. Liu, A. Liashenko, P. Piskorz, I. Komaromi, R. L. Martin, D. J. Fox, T. Keith, M. A. Al-Laham, C. Y. Peng, A. Nanayakkara, M. Challacombe, P. M. W. Gill, B. Johnson, W. Chen, M. W. Wong, C. Gonzalez, J. A. Pople, GAUSSIAN 03 (Revision E.01), Gaussian, Inc., Wallingford, CT, 2004.
30. M. Morita, Y. Asai, N. Yoshimoto, M. Ishikawa, *J. Chem. Soc., Faraday Trans.*, 1998, **94**, 3451–3456.
31. D. Brouillette, G. Perron, J. E. Desnoyers, *J. Solution Chem.*, 1998, **27**, 151–182.
32. K. Kuratani, N. Uemura, H. Senoh, H. T. Takeshita, T. Kiyobayashi, *J. Power Sources*, 2013, **223**, 175–182.
33. M. Ishikawa, M. Morita, M. Asao, Y. Mastuda, *J. Electrochem. Soc.*, 1994, **141**, 1105–1108.
34. A. Allerhand, H. S. Gutowsky, J. Jonas, R. A. Meizner, *J. Am. Chem. Soc.*, 1966, **88**, 3185–3194.
35. K. G. Orrel, V. Šik, D. Stephenson, *Prog. Nucl. Mag. Res. Sp.*, 1990, **22**, 141–208.
36. L. Helm, A. E. Merbach, *Chem. Rev.*, 2005, **105**, 1923–1960.
37. K. Hayamizu, Y. Aihara, S. Arai, C. Martinez, *J. Phys. Chem. B*, 1999, **103**, 519–524.
38. K. Hayamizu, E. Akiba, T. Bando, Y. Aihara, *J. Chem. Phys.*, 2002, **117**, 5929–5939.
39. H. Tokuda, S.-J. Baek, M. Watanabe, *Electrochemistry (Tokyo, Jpn.)*, 2005, **73**, 620–622.
40. H. Tokuda, K. Hayamizu, K. Ishii, M. A. B. H. Susan, M. Watanabe, *J. Phys. Chem. B*, 2005, **109**, 6103–6110.
41. H. Tokuda, K. Ishii, M. A. B. H. Susan, S. Tsuzuki, M. Watanabe, *J. Phys. Chem. B*, 2006, **110**, 2833–2839.
42. H. Tokuda, S. Tsuzuki, M. A. B. H. Susan, K. Hayamizu, M. Watanabe, *J. Phys. Chem. B*, 2006, **110**, 19593–19600.
43. M. Yoshizawa, W. Xu, C. A. Angell, *J. Am. Chem. Soc.*, 2003, **125**, 15411–15419.
44. M. S. Miran, H. Kinoshita, T. Yasuda, M. A. B. H. Susan, M. Watanabe, *Phys. Chem. Chem. Phys.*, 2012, **14**,

5178–5186.

45. M. Takeuchi, Y. Kameda, Y. Umebayashi, S. Ogawa, T. Sonoda, S. Ishiguro, M. Fujita, M. Sano, *J. Mol. Liq.*, 2009, **148**, 99–108.
46. J. Dupont, *J. Brazil. Chem. Soc.*, 2004, **15**, 341–350.
47. J. Hunger, A. Stoppa, R. Buchner, G. Hefter, *J. Phys. Chem. B*, 2008, **112**, 12913–12919.
48. S. Schrödle, G. Annat, D. R. McFarlane, M. Forsyth, R. Buchner, G. Hefter, *Chem. Commun.*, 2006, 1748–1750.
49. J. Wang, L. Zhang, H. Wang, C. Wu, *J. Phys. Chem. B*, 2011, **115**, 4955–4962.
50. J.-L. M. Abboud, R. Notario, *Pure. Appl. Chem.*, 1999, **71**, 645–718.
51. C. F. Riadigos, R. Iglesias, M. A. Rivas, T. P. Iglesias, *J. Chem. Thermodynamics*, 2011, **43**, 275–283.
52. K. Izutsu, *Electrochemistry in Nonaqueous Solutions, Second, Revised and Enlarged Edition*; Wiley-VCH Verlag GmbH & Co. KGaA, Weiheim, 2009.
53. R. A. Robinson, R. H. Stokes, *Electrolyte Solutions*; Dover Publications, 1970.
54. J. O. M. Bockris, A. K. N. Reddy, *Modern Electrochemistry I: Ionics*; Springer, 1998.
55. S. Tsuzuki, W. Shinoda, S. Seki, Y. Umebayashi, K. Yoshida, K. Dokko, M. Watanabe, *ChemPhysChem*, 2013, **14**, 1993–2001.

Table of Contents

Equimolar complex of pentaglyme (G5) and sodium bis(trifluoromethanesulfonyl)amide (Na[TFSA]) behaves like room-temperature ionic liquids and is a promising electrolyte for Na-ion batteries.

